ELSEVIER

Chemical Engineering Journal 74 (1999) 67–75

Chemical Engineering Journal

An order(*N*) tight-binding molecular dynamics study of intrinsic defect diffusion in silicon

Bruce W. Roberts[a,*], Weiwei Luo[b], Kurt A. Johnson[a], Paulette Clancy[b]

[a]*Laboratory of Atomic and Solid–State Physics, Cornell University, Ithaca, NY 14853–2501, USA*

[b]*School of Chemical Engineering, Cornell University, Ithaca, NY 14853, USA*

Abstract

We present calculations of the intrinsic vacancy and interstitial diffusivities, D_V and D_I, in silicon using order(*N*) tight-binding molecular dynamics simulations. Vacancy diffusion was found to occur rapidly, with a diffusivity of around 10^{-4} cm^2/s in the temperature range 900–1200°C. Interstitial diffusion was found to be a factor of 10–100 times slower than vacancy diffusion, being on the order of 10^{-5} cm^2/s for the same temperature range. These diffusivities have the same order of magnitude as previous molecular dynamics calculations performed with both classical and Car-Parrinello models. The interstitial diffusion was found to occur via two different paths, one involving motion of a single interstitial down the open (110) channels in the lattice, and another involving an intermediate ⟨110⟩ split interstitial which facilitates the interstitial crossing from one (110) channel to another. Within the tight-binding model we use, the split interstitial path is more important than drift of a single interstitial at higher temperatures (here, above around 1000°C). The reverse is true below this temperature, with few, if any, formations of split interstitials and a diffusion dominated by traversal down the open channels of the lattice. New LDA data shows that the energetic advantage of the split interstitial over the tetrahedral interstitial is smaller than previously calculated, lending credence to the tight-binding results. The split interstitials were found to be relatively long-lived (in some cases, lifetimes in excess of 15 ps), even in a potential that favors tetrahedral interstitial formation. In order to perform these calculations, we developed a constant N_{elec} version of the forces in the Goedecker and Colombo O(*N*) tight-binding algorithm originally written for systems with a constant chemical potential. Omission of this correction can lead to errors approaching 40% in the forces.

Keywords: Intrinsic defect diffusion; Silicon; Tight-binding molecular dynamics

1. Introduction

Atomic diffusion of defects is important in determining the equilibrium, transport, and kinetic properties of materials, especially when processed at high temperatures [1,2]. In silicon, intrinsic defects control the migration of impurities and dopant atoms. Understanding the detailed kinetics of these diffusional processes is critical for the control and fabrication of modern electronic devices. Indeed control of dopant atom diffusion is a fundamental limitation for the processing of semiconductor devices, ultimately controlling the sizes of features that can be created under typical processing temperatures [3]. In addition, as the scale of the structures in electronic devices approaches the atomic level (0.10 μm is the current SIA Roadmap goal for feature sizes), it becomes increasingly important to understand the atomic-scale fundamentals of diffusion. Aside from the interest in diffusion fundamentals, knowledge of quantities such as diffusivities and migration energies is important as inputs to continuum modeling packages such as SUPREM [4] and particularly to newer simulation tools such as Stanford's PDE solver ALAMODE [5].

Experimental results for native point defects (vacancies and interstitials) in silicon yield intrinsic diffusion constants that are several orders of magnitude smaller than existing simulation results.[1] Recent experimental studies cite vacancy diffusivities [7] of around 10^{-7}–10^{-8} cm^2/s, whereas atomic-scale simulations of point defect diffusivities [8–10] (admittedly, at much higher temperatures) produce values around 10^{-4} cm^2/s. However, recent EPR data quotes values "approaching LDA (local density approximation, a quantum mechanical description) values" [11]. Results for interstitial diffusion show a larger discrepancy between experiment and atomic-scale simulation. The clo-

*Corresponding author. Fax: +1-607-255-9166; e-mail: tpc@cheme.cornell.edu

[1]See for example [6]. The review by Fahey, Griffin and Plummer, Ref. [1], is another valuable resource.

1385-8947/99/$ – see front matter
PII: S1385-8947(99)00062-5

sest comparison for interstitial diffusion rates to date are those of Privitera et al. [12] of "no slower than 10^{-10} cm^2/s with atomic-scale data of around 10^{-6} cm^2/s. While all the sources of these discrepancies between experiment and simulation are unclear, the existence in real materials of vacancy and interstitial traps (present in real materials: absent in virtual silicon) clearly plays a role. For instance, carbon is known to be an interstitial trap [13]; its presence retards the diffusion of boron (an "interstitial diffuser") in Si. Oxygen has been suggested as a potential vacancy trap [14]. It is possible that there are point defect–point defect traps, but experimental verification of such a suggestion would be extremely difficult and has not yet been attempted. Another factor in the discrepancy between experiment and simulation must be the accuracy of the atomic models, but this question is also unresolved and serves as a key motivation for the work to be presented here.

Previous atomic-level simulations of intrinsic point defects in Si include studies [8,9,15,16] using the Stillinger–Weber (SW) classical models [17], and ab initio Car-Parrinello molecular dynamics calculations [10]. The SW simulations, performed for comparatively large systems (576 atoms) for "long" times (300 ps), provide accurate estimates of the diffusion constants within the constraints (i.e. the realism) of that model. The ab initio Car-Parrinello results suggest similar order-of-magnitude estimates of the diffusivities to the SW results, but the greater realism of the model is hampered by the computational burden in calculating diffusivities even for small (64-atom) systems run for short timescales (<20 ps). Thus one study was hampered by the realism of the model and the other by constraints of size and timescales.

We chose to use an approximate method, the tight-binding model [18], that is more accurate in energy determinations (and hence slower) than the SW model, but faster (though somewhat less accurate in measuring the energy surface) than the ab initio method. The goal here was to determine the diffusivities of vacancies and interstitials, D_V and D_I, respectively, using a larger system size for longer timescales than are possible using an ab initio method. In this way, the order of magnitude of diffusivities from another atomic-scale model could confirm or deny the apparent consensus of simulation results, and perhaps, shed some light into the discrepancy of atomic-scale results with experiments.

There has been one previous tight-binding simulation of point defect diffusivities [19]. But there are several differences between the approach presented here and that of Tang et al. [19]. The most important difference is that their tight-binding model was due to Kwon et al. [20]. The parameterization of the Kwon model was chosen to reproduce the LDA results that show a preference for the formation of (110) split interstitials over tetrahedral interstitials. In contrast, the model used here, that due to Goodwin, Skinner and Pettifor (GSP) [21], was not fitted to defect properties. In consequence, GSP slightly favors the formation of tetrahedral interstitials and hence is an interesting counterpoint to the Kwon model. The relative balance of time spent in the split and tetrahedral positions during interstitial diffusion has never been identified for either the Kwon or GSP model. Hence it is still unclear how sound it is to choose a tight-binding model based largely on its ability to demonstrate the preferred location of the interstitial. This point will be developed in the paper that follows. Secondly, we provide here an order(N) linear-scaling algorithm that is applicable to the study of defect diffusion. This enables us to make some comments as to the effectiveness of a fast O(N) code in comparison to traditional O(N^3) tight-binding codes.

Our paper is organized as follows. In Section 2 we provide a summary of the simulation method we use. Section 3 presents results for the diffusivities for vacancies and interstitials, as well as a discussion of the interstitial diffusion mechanism. Our conclusions are given in Section 4. Appendix A describes the O(N) method used, including the correction that we derived to give correct forces around defects.

2. Simulation method

The method used here for simulations of self diffusion in silicon is tight-binding molecular dynamics (TBMD) [22–24]. This method involves making approximations from an exact quantum mechanical description in order to obtain an algorithm that is computationally tractable. It is much faster than (almost exact) density functional methods, and more accurate in terms of bonding and electronic structure than classical potentials.

Even with the speed-up gained through the use of tight-binding over density functional methods, large systems can still take a long time to calculate for one time step (for example, 216 atoms can take up to 20 min per time step on a fast serial workstation). This is because the basic solution method depends on calculating the eigenvalues and eigenvectors of the Hamiltonian matrix. Such a process scales as O(N^3), where N is the number of atoms in the system. Recently, methods have been developed which make approximations to improve the scaling of the solution method to O(N) [25,26]. We use one such linear-scaling method, developed by Goedecker and Colombo [27,28]. This particular O(N) method is explicitly parallelizable, and allows us to take advantage of parallel computers such as the IBM SP2. We review this method in Appendix A and also present an addition to the method that we have developed to handle a constant number of electrons, N_{elec}, as opposed to constant chemical potential μ, during force calculations. This addition is essential in order to obtain accurate results for the forces around defects, which are, in turn, necessary for the correct description of diffusion in the tight-binding model. Failure to include this new correction was found to lead to errors of around 40% in the forces.

To estimate the errors introduced due to the O(N) approximations, we compared the formation energies of unrelaxed vacancies and interstitials in 64±1 atom unit cells in the O(N) method and by direct diagonalization of the Hamiltonian. For the vacancy, direct diagonalization at the Γ point yields a formation energy of 5.02 eV [29], while the O(N) algorithm gives 4.94 eV (−1%). For the interstitial, the direct diagonalization result is 6.42 eV [29] and 6.48 eV for the O(N) code (+1%). The error in these results is certainly less than the systematic errors made in the tight-binding approximation itself. Typical deviations of tight-binding formation energies from ab initio results are on the order of 1 eV. However, we expect energy differences (and hence forces) to have smaller systematic errors.

For the tight-binding molecular dynamics runs, we used an NVT (constant temperature) ensemble, and a system size of 216±1 atoms (3×3×3 cubic unit cells) with periodic boundary conditions. The choice of system size is a trade-off between simulation time and finite size effects due to defect–defect interactions. We have also performed some shorter duration simulations (approximately 3 ps) for smaller systems (64±1 atoms), and we find similar results for the diffusivities (although with much larger statistical errors). We used a time step of 1.0 fs, which was found to give an appropriate degree of energy conservation. The lattice constant of the perfect solid is 5.42981 Å.

A system size of 216 atoms also reduces the amount of systematic error in formation energies of defects when compared to the same quantities in a 64-atom cell. Typical differences between formation energies in a 216-atom cell and a 64-atom cell are on the order of 0.1–0.3 eV. This is too large a discrepancy to allow, since continuum process simulators like ALAMODE require formation energies accurate to about 0.1 eV. The differences between a 512-atom cell and a 216-atom cell are smaller [29,30], though the difference depends on the precision with which the calculations are carried out (e.g. the number of k-points used). The difference is small enough that, fortunately, the smaller 216-atom result is acceptable.

The TBMD simulations consisted of running a system with a vacancy or interstitial for an appropriate length of time. We found that the diffusivity of a vacancy can be reasonably accurately determined by two simulation run times of around 30 ps (30 000 time steps) each, taking data every 50 fs after an initial equilibration period of around 1 ps. The diffusivity of an interstitial at high temperature can be reasonably accurately determined by two 30 ps runs too (see Fig. 1). At lower temperatures, it would be prudent to run the simulation for as long as practical. Such runs take very considerable computational resources. Even using the order(N) code on 16 processors of the IBM SP2, we needed 225 h of CPU time per processor to complete 180 ps. The data were found to be insensitive to the period of the initial equilibration time (in the range 100–1000 fs). Typical phonon frequencies in silicon are around 1–17 THz. This corresponds to a timescale of approximately 50–1000 fs, so we expect to be able to resolve lattice vibrations and rearrangements using the chosen time slice of 50 fs.

Results were compiled for five different temperatures for both the vacancy and the interstitial: 900°C, 975°C, 1050°C,

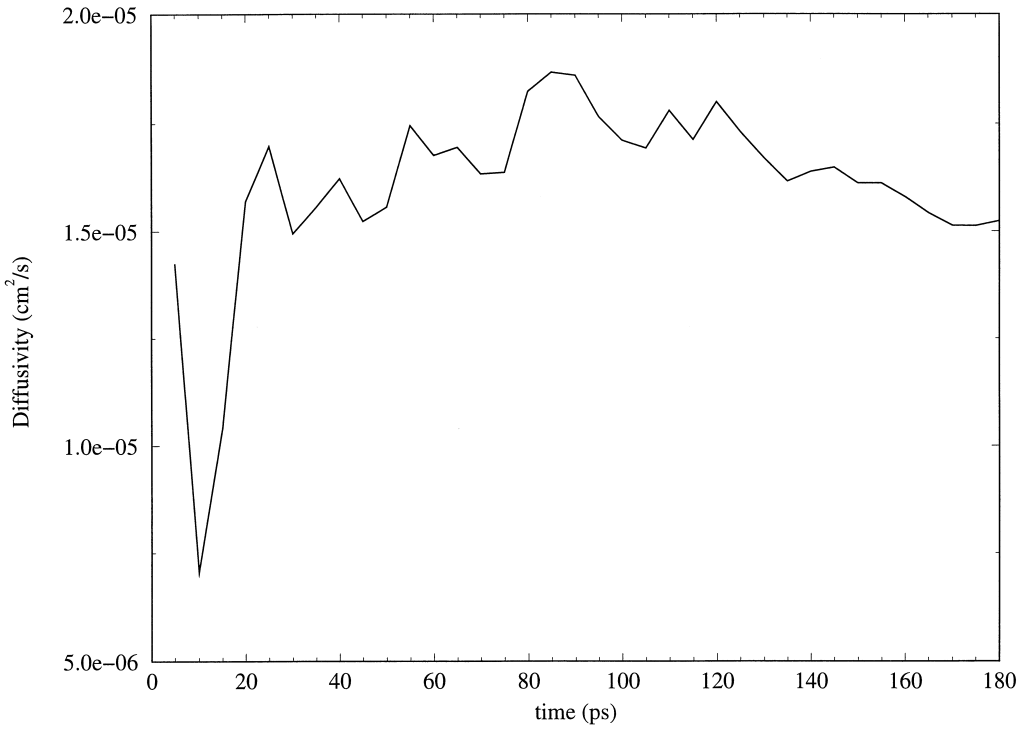

Fig. 1. Evolution of the diffusivity of an interstitial as a function of time. Results are averaged over two separate runs both at 1200°C.

1125°C and 1200°C. Each run at a particular temperature was repeated for two different initial configurations of the system, starting from an appropriate velocity distribution for that temperature and a slightly distorted lattice. All the vacancy runs were continued for two runs of 30 ps each. The interstitial runs at the lowest four temperatures were terminated after two runs of 30 ps. Two long simulations were performed at 1200°C; each run took 180 ps. Resource constraints did not allow us to take all five temperatures out to 100 ps. But from Fig. 1, we estimate that the results after two 30 ps runs are accurate at high temperatures. We shall show that the TBMD results obtained here compare favorably to other atomic-scale calculations.

The calculation of the diffusivities was made by partitioning each run into a number of time intervals Δt, and then averaging the diffusion results over all these time origins. Typically Δt was 300 fs and 100 time origins were considered. The effect on the diffusivities of changing Δt was to increase the error. Larger Δt values tended to have larger statistical errors, while smaller Δt values tended to give larger deviations from Arrhenius behavior when several temperatures were considered. This is likely to be due to the smaller time intervals not giving the system time to adequately sample the full energy surface on which the atoms move in the diffusion process.

3. Results

The diffusion constant of a vacancy or interstitial was calculated using the well known Einstein formula:

$$D = \frac{[\vec{x}(t) - \vec{x}(0)]^2}{6t}, \quad (1)$$

which is exact in the limit $t \to \infty$, and where $\vec{x}(t)$ is the location of the defect at time t. During these simulations it is essential to keep track of the location of any vacancies and/or interstitials present in the system. The criteria for locating vacancies and interstitials are given in the sections that follow. In these studies it was also necessary to determine when a defect crossed a periodic boundary. This is because the calculation of the diffusion constant involves knowing the absolute vector distance from the starting point; some of our simulation runs were long enough that this was an issue.

3.1. Diffusion of vacancies

The location of vacancies was accomplished by considering the distance of all the atoms from the perfect lattice sites. If there is no atom within a cut-off distance, chosen here to be a generous 1.0 Å, of a perfect lattice site, then we determine this lattice site to be empty and hence the location of a vacancy. This allowed us to keep track of the hopping of the vacancies, and determine the number of hops in a particular run.

Typically, a vacancy hop takes 150–200 fs, which is consistent with phonon frequencies mentioned above. During this time, one of the four atoms nearest the vacancy will move to occupy the lattice site of the vacancy, leaving a new unoccupied lattice site. The typical number of vacancy hops is in the range 30–45 per 30 ps for the temperatures we considered.

Results for the diffusivities of vacancies and interstitials are shown in Fig. 2. An Arrhenius plot of the relationship of D_V and D_I, $\log_{10}D$ versus $1/T$ showed a straight line for both defects. This implies that the diffusion constants are given by the form $D=D_0\,e^{-\Delta/kT}$, where Δ is a migration energy barrier. The TBMD data for the vacancy diffusivity gave rise to a migration energy, $\Delta=0.13$ eV, and a prefactor $D_0=4.1\times10^{-4}$ cm^2/s. Previous statics calculations from our group for the tight-binding model gave a migration energy of approximately 0.1 ± 0.25 eV [31]. Using Kwon's model, Tang et al. [19] obtain a similar value of 0.1 eV.

We can compare these results to those obtained from SW and ab initio simulations. The ab initio simulations give only an order of magnitude estimate of $D=10^{-4}$ cm^2/s for both the vacancy and interstitial diffusivities [10]. Our results ($D=(1.3\pm0.3)\times10^{-4}$ cm^2/s for 900–1200°C) certainly agree with this rough estimate. The SW simulations [9] calculate a migration energy of 0.46 eV, and a prefactor of 1.70×10^{-3}, with no estimate of the errors. While our results are somewhat different from the SW results, they still compare reasonably well given the different models used. SW statics calculation [15,16] yield a migration energy of 0.43 eV. From the prefactor and migration energy in Tang et al.'s paper [19], the diffusivity was calculated as being in the range 4.4×10^{-5}–5.4×10^{-5} cm^2/s for 900–1200°C.

3.2. Diffusion of interstitials

In order to calculate the diffusivity of an interstitial, the perfect lattice was "seeded" with a single tetrahedral interstitial. We followed the location of this atom as it moves down the open channels formed by the diamond cubic lattice. However, the presence of this interstitial can lead to the formation of a $\langle 110 \rangle$ split interstitial (SI). The original interstitial atom in this SI pair can sometimes share a lattice site with a second, previously substitutional, atom (as shown in Fig. 3). If an exchange event occurs, the second atom (the one formerly occupying the substitutional site) may be forced from its lattice site and become a new tetrahedral interstitial. In such a case, it is important for the code to recognize the change of identity of the interstitial atom and track the new atom as it diffuses through the lattice as if it were the original interstitial atom. Otherwise the diffusivity will be calculated incorrectly. Of course, interstitial exchange events can lead to substantial jumps in the position of the active interstitial and hence lead to an enhanced diffusivity. We observed that the time spent in the split interstitial arrangement as compared to time spent

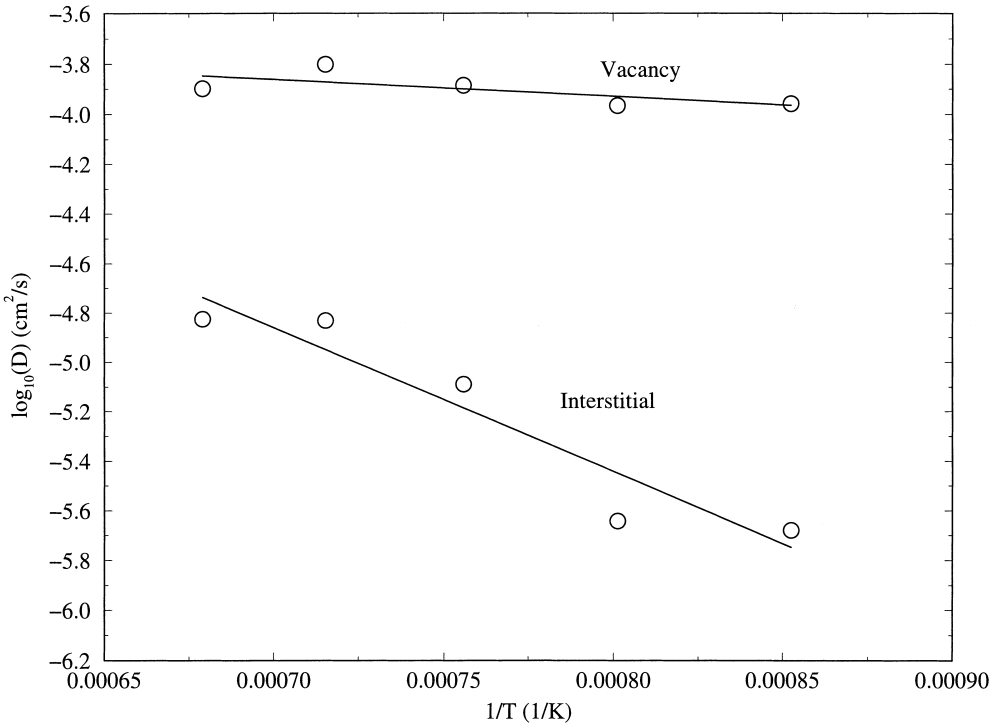

Fig. 2. Diffusivities for vacancies and interstitials. The solid lines represent fits to the form $D=D_0\,e^{-\Delta/kT}$.

wandering down the open channels of the Si lattice was roughly 45% as a SI compared to 55% as a migrant interstitial.

We observed many events during the simulations in which formerly tetrahedral interstitials formed split interstitials leading to the exchange of one interstitial atom for another. We also observed the spontaneous formation of a new interstitial, typically in the vicinity of an existing split interstitial pair. On rare occasions we saw the direct transformation of one split interstitial pair into another split interstitial pair (i.e. a move involving three neighboring atoms).

Table 1 shows the total number of such exchange events, and the total number of split interstitials formed for the five temperatures studied. Data for the average of the two 30 ps runs of the 1200°C run were used in order to make a fair comparison to the other temperatures. In many of the dissociations of the SI pairs, the original interstitial atom returned to the tetrahedral interstitial site. It is also interesting to note that the frequency of exchange events and the formation of SI pairs depend on the temperature. The exchange mechanism plays a larger role at higher temperatures, at least as predicted by the tight-binding model. A temperature-dependent crossover in diffusion mechanism

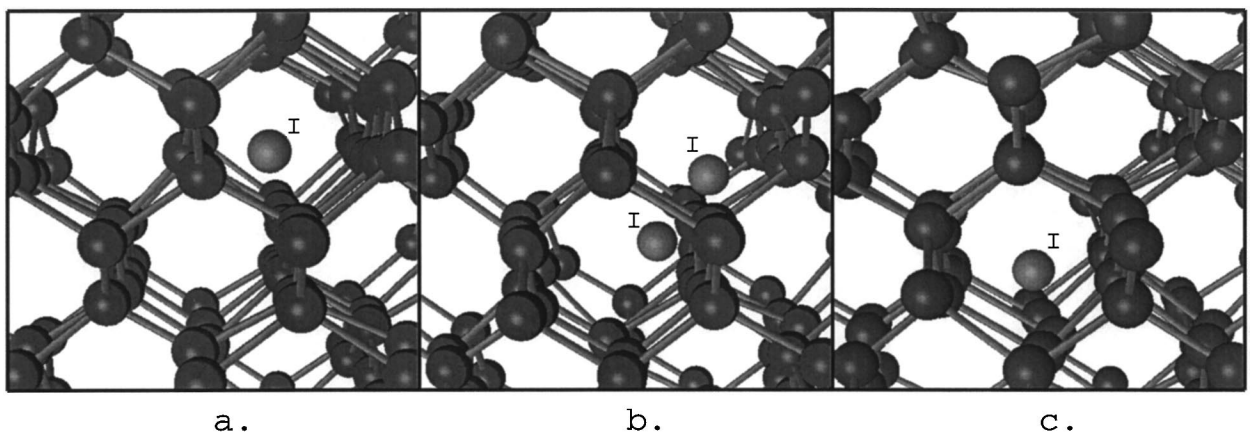

Fig. 3. The exchange event for diffusion of an interstitial. The interstitial atoms have been labeled with the letter **I** for clarity. (a) The initial interstitial, looking down a ⟨110⟩ channel; (b) the ⟨110⟩ split interstitial formed from the original interstitial and a lattice atom; (c) the new interstitial in a different ⟨110⟩ channel after the exchange event.

Table 1
Split interstitial formation, averaged over two runs of 30 ps each

Temperature (°C)	Si pairs formed	Exchange events
900	1.5	0
975	0.5	0
1050	3.5	2.0
1125	5.5	1.5
1200	10.5	2.5

for interstitials has been suggested by several researchers (e.g. see [36]), and our results are suggestive that there indeed might be processes important to diffusion at high temperature that are ''frozen out'' at lower temperatures. We are continuing these interstitial runs from 60 ps to over 100 ps to ensure that this temperature dependence of the dominant mechanism is not related to the length of our runs.

Fig. 2 also provides insight concerning the nature of interstitial diffusivity. Two things are immediately apparent: D_I is one to two orders of magnitude smaller than D_V, and it too conforms to an Arrhenius behavior, $D_I = D_0\, e^{-\Delta/kT}$. This data estimates the barrier to migration to be $\Delta = 1.2$ eV, and the prefactor $D_0 = 0.165$ cm^2/s. Again we can compare these results to those obtained from SW and ab initio simulations. The previous ab initio simulations give only an order of magnitude estimate of $D = 10^{-4}$ cm^2/s for the interstitial diffusivities [10]. Our results are about an order of magnitude slower than the LDA results ($D = 0.2$ to 1.5×10^{-5} cm^2/s for 900–1200°C). Results from the other tight-binding study of interstitial diffusion (by Tang et al. [19]) are in reasonable accord with our result (e.g. one can calculate their value for D at 1200°C to be 0.32×10^{-5} cm^2/s). The SW simulations [9] calculate a migration energy of 0.94 eV, and a prefactor of 1.76×10^{-2}. Tang's [19] results give a migration energy barrier of 1.37 eV and $D_0 = 0.158$ cm^2/s, starting from a split interstitial pair. We can also compare the interstitial results to previous statics calculations. SW statics yield a migration barrier of roughly 1.7 eV [15,16], while the tight-binding statics give a barrier of 0.7 ± 0.25 eV [31].

It is known that the GSP tight-binding model (as originally parameterized) and local density approximation (LDA) methods disagree regarding the location of the most stable Si self-interstitial. The LDA predicts the split interstitial to be more stable, while the original GSP tight-binding model shows a slight preference for the tetrahedral location. Given this information, and the key role played by split interstitials in interstitial diffusion as witnessed by the TBMD results in this paper, we felt it was necessary to re-check the LDA results. For this purpose, ab initio total-energy pseudopotential calculations within the LDA were performed with a plane-wave basis set [32–35]. The silicon pseudopotential was norm-conserving with a cut-off radius of 1.80 bohr. Defects were introduced into a 64-atom cubic unit cell with 65 and 63 atoms comprising the interstitial and vacancy calculations, respectively. A plane-wave energy cut-off of 300 eV was sufficient to converge the total energy of these systems (by comparison with calculations performed at 600 eV) to 0.02 eV/atom, with defect formation energies correspondingly converged to 0.02 eV. k-point selection consisted of both $2\times2\times2$ and $4\times4\times4$ Monkhorst-Pack grids with defect energies found to be converged to within 0.1 and 0.01 eV for the respective grid densities. An $8\times8\times8$ grid was utilized in a defect-free 64-atom silicon cell, and the total energy differed by only 0.001 eV from the $4\times4\times4$ grid which indicates the well-converged status of the $4\times4\times4$ grid. Ionic positions of all atoms in the cell were relaxed using a conjugate gradient method with forces reduced below 0.01 eV/bohr which lead to total energies converged to better than 0.001 eV with respect to the force cut-off.

The precision provided by such a dense k-point grid and force cut-off allows a much finer comparison between the tetrahedral and split interstitials than virtually all previous calculations. Results, accurate to within 0.02 eV with respect to all of the numerical parameters, are shown in Table 2. They confirm the earlier LDA results indicating a preference of the split interstitial location to that of the tetrahedral one, but the difference is significantly closer than implied by the earlier LDA results. The new results show only a weak preference between the two locations and makes the deficiencies in the tight-binding predictions less critical. The energetic preference for T-interstitials in the GSP tight-binding method does not appear to seriously impede the formation of split interstitials, as evidenced by the TBMD results shown here. The LDA preference for split interstitials magnifies the likelihood that the TBMD results here are correct in their implication of the importance of SIs in interstitial diffusion mechanisms. We see no reason to add any ad hoc energy band gap correction in the manner employed by Tang et al. It is interesting to note that their LDA values (before the band gap correction was added to the formation energy of the T-interstitial) also confirm the close energetics between T- and split interstitials [42]. Use of a generalized gradient correction would not affect the formation energies given here (GGA would change the

Table 2
Formation energies for vacancies and self-interstitials in Si from LDA and tight-binding (TB) methods (values given in eV)

Approach (reference)	Vacancy	Tetrahedral interstitial	Split interstitial
LDA (Zhu [37])	–	4.6[a]	3.2
LDA (Blöchl et al. [10])	4.1	–	3.3
LDA[b] (Clark and Ackland [38])	–	Unstable	2.16
LDA (Tang et al. [42])	–	3.5	3.2
LDA (Mercer et al. [43])	3.6	–	–
LDA ($2\times2\times2$ MP grid; this work)	3.57	3.30	3.16
LDA ($4\times4\times4$ MP grid; this work)	3.74	3.29 ± 0.02	3.26 ± 0.02
TB (steepest descents statics [39])	3.15	4.7 ± 0.3	5.0 ± 0.3

[a] A 1.3 eV band gap ''correction'' was been added by the author, Zhu, to the total energy calculated by the LDA calculation. The correction is calculated as twice the difference between the real band gap for Si and that predicted by LDA. See their paper for details.
[b] Note that a short cut-off (150 eV) was used by these authors. Cut-offs of 300–500 eV are typical and preferable.

absolute values of the energies but would not alter the energy difference needed for E_f).

4. Conclusions

We have calculated diffusivities for intrinsic defects in silicon using tight-binding molecular dynamics. The order of magnitude of the vacancy and interstitial diffusivities are consistent with previous classical and ab initio dynamic simulations and with statics results. Our calculations eliminate any serious concern that limitations of realism of the SW results or brevity of the CP results have contributed to the high values obtained for diffusion of intrinsic defects in Si. Thus, all atomic-level simulations of diffusivities performed to date remain significantly larger than experimental results. Since computer ''silicon'' is a perfectly clean and defect-free system (apart from the single seeded defect) we believe that this points to the importance of trapping mechanisms in real materials.

Given this single unresolvable issue, we contend that intrinsic diffusivities of vacancies and interstitials are remarkably fast. Vacancies diffuse significantly faster than interstitials (by one to two orders of magnitude) in the temperature regime 900–1200°C. We have also quantified the mechanism for interstitial diffusion in terms of its two components: drift down the open (100) channels and formation of $\langle 110 \rangle$ split interstitials. At around 1200°C, the interstitial spends roughly 55% of its time as a wandering T-interstitial and around 45% of its time bound up as a $\langle 110 \rangle$ split interstitial. Within a tight-binding description of the interatomic forces, the dominant mechanism changes from one of single interstitial drift at low temperatures to one of exchange processes with lattice atoms through intermediate $\langle 110 \rangle$ split interstitials at higher temperatures. New LDA results confirm the importance of the split interstitial defect while showing that the difference between T- and split interstitial formation energies is small.

Acknowledgements

The authors would like to thank S. Goedecker, A.L.K. Roberts, and M.O. Thompson for their useful discussions. This work was funded by the National Science Foundation under grant DMR-95-20315. We also thank the Cornell Center for Materials Research and the Cornell Theory Center for the use of their computational resources.

Appendix

O(N) tight-binding and constant N forces

A.1 Order(N) tight-binding

In this section, we summarize the O(N) method that we use for our calculations. Further details can be found in [27,28].

In the tight-binding method, the total energy can be written as

$$E_{\text{tot}} = E_{\text{kin}} + E_{\text{pot}} + E_{\text{bs}}. \tag{A.1}$$

The method begins by rewriting the total energy in equation as

$$E_{\text{tot}} = E_{\text{kin}} + E_{\text{pot}} + \sum_i \varepsilon_i f\left(\frac{\varepsilon_i - \mu}{\tau}\right), \tag{A.2}$$

where the function f is defined as

$$f(x) = \frac{1}{1 + \mathrm{e}^x}. \tag{A.3}$$

This is the Fermi function, and τ plays the role of a fictitious electron temperature, and μ a chemical potential. We would like to emphasize that this is not the actual temperature, but rather an approximation that allows us to obtain an O(N) method.

The goal is to calculate the electron band-structure energy contribution without having to diagonalize the Hamiltonian H. To this end we define the Fermi matrix:

$$F = f\left(\frac{H - \mu}{\tau}\right). \tag{A.4}$$

Using this, the band-structure energy is given by

$$E_{\text{bs}} = \sum_i \varepsilon_i f\left(\frac{\varepsilon_i - \mu}{\tau}\right) = \text{Trace}[HF] = \sum_{n\alpha} \langle \phi_{n\alpha} | HF | \phi_{n\alpha} \rangle. \tag{A.5}$$

where the $|\phi_{n\alpha}\rangle$ are the atomic orbital basis functions.

Next, we approximate the Fermi matrix as a polynomial in H, $F \approx p_{\mu,\tau}(H)$. We use for this polynomial a series of Chebychev polynomials $T_m(H)$:

$$p_{\mu,\tau}(H) = \frac{c_0(\mu,\tau)}{2} I + \sum_{m=1}^{n_{pl}} c_m(\mu,\tau) T_m(H). \tag{A.6}$$

The Chebychev polynomials are defined by the recursion relations:

$$\begin{aligned} T_0(H) &= I \\ T_1(H) &= H \\ T_{m+1}(H) &= 2HT_m(H) - T_{m-1}(H). \end{aligned} \tag{A.7}$$

We can use these relations to calculate one column of $T_m(H)$, $|t^m_{n\alpha}\rangle$:

$$\begin{aligned} |t^0_{n\alpha}\rangle &= |\delta_{n\alpha}\rangle \\ |t^1_{n\alpha}\rangle &= H|\phi_{n\alpha}\rangle \\ |t^{m+1}_{n\alpha}\rangle &= 2H|t^m_{n\alpha}\rangle - |t^{m-1}_{n\alpha}\rangle. \end{aligned} \tag{A.8}$$

From here we can calculate a ''localized orbital'':

$$|f_{n\alpha}\rangle = F|\phi_{n\alpha}\rangle \approx p_{\mu,\tau}(H)|\phi_{n\alpha}\rangle = \frac{c_0(\mu,\tau)}{2}|t^0_{n\alpha}\rangle + \sum_{m=1}^{n_{pl}} c_m(\mu,\tau)|t^m_{n\alpha}\rangle. \tag{A.9}$$

The localized orbital $|f_{n\alpha}\rangle$ decays as we move away from the nth atom. In semiconductors this decay is exponential. Once we have this localized orbital, one further matrix-vector multiply, one dot product, and a sum over states gives the band-structure energy.

So far, we have presented an approximate method for calculating the band-structure energy. How long does this process take? Each matrix-vector multiplication takes an amount of time that scales as N_{atoms}^2 to perform, and there are approximately n_{pl} matrix-vector multiplications, so the time t for one step in the computation scales as $t \sim N_{\text{atoms}}^2 n_{pl}$. As written, the algorithm is O(N^2). In order to obtain an O(N) algorithm, we need to introduce a further approximation. Because of the exponential decay of the localized orbital $|f_{n\alpha}\rangle$, we can introduce a cut-off region beyond which we do not perform calculations when doing the matrix multiplications necessary to generate F. Instead of the matrix multiplications taking time $t \sim N_{\text{atoms}}^2$, they take $N_{\text{atoms}} N_{\text{loc}}$, where N_{loc} is the typical number of atoms in the cut-off region, which is fixed as we increase N_{atoms}. Doing this yields a linear-scaling algorithm with computation time of $t \sim N_{\text{atoms}} N_{\text{loc}} n_{\text{pl}}$.

An additional advantage of this algorithm is that it can be used efficiently on parallel computers. To see this, note that one sequence of columns $|t_{n\alpha}^m\rangle$, $m = 0, \ldots, n_{pl}$ is completely independent of another sequence $|t_{n'\alpha'}^m\rangle$, $m = 0, \ldots, n_{pl}$. We can then calculate the localized orbitals for different nuclei on different processors of a parallel computer. The time to compute all the necessary orbitals is reduced by a factor of $1/N_{\text{processors}}$.

A.2 Force correction for constant N_{elec}

As presented in [27,28], the O(N) algorithm calculates forces assuming a constant chemical potential. We have found that in order to get correct forces around defect structures it is important to calculate these forces assuming a constant number of electrons. This section gives a method we have developed for doing such a calculation.

We want to calculate the forces from the band-structure energy E_{bs} given in (Eq. (A.5)), assuming a constant number of electrons. The total number of electrons N in the system can be calculated from

$$N = \sum_i f\left(\frac{\varepsilon_i - \mu}{\tau}\right) = \text{Tr}[F]. \tag{A.10}$$

We are particularly interested in the forces on one atom n located at $\vec{R}_n$ due to the electron band-structure energy. We can write the force as

$$\vec{f}_n = -\frac{\partial E_{\text{bs}}}{\partial \vec{R}_n} = -\text{Tr}\left[\frac{\partial H}{\partial \vec{R}_n} F + H \frac{\partial F}{\partial \vec{R}_n}\right], \tag{A.11}$$

where we have used the Hellmann–Feynman theorem [40] to write $(\partial/\partial \vec{R}_n)\text{Tr}[HF] = \text{Tr}[(\partial/\partial \vec{R}_n)HF]$. Taking the derivative for F yields

$$\frac{\partial F}{\partial \vec{R}_n} = f'\left(\frac{H-\mu}{\tau}\right)\frac{1}{\tau}\left(\frac{\partial H}{\partial \vec{R}_n} - \frac{\partial \mu}{\partial \vec{R}_n}\right), \tag{A.12}$$

where in our approximation

$$f'\left(\frac{H-\mu}{\tau}\right)\frac{1}{\tau} = p'_{\mu,\tau}(H) \tag{A.13}$$

This gives a force

$$\vec{f}_n = -\text{Tr}\left[\frac{\partial H}{\partial \vec{R}_n}\left(p_{\mu,\tau}(H) + H p'_{\mu,\tau}(H)\right)\right] + \frac{\partial \mu}{\partial \vec{R}_n}\text{Tr}\left[H p'_{\mu,\tau}(H)\right]. \tag{A.14}$$

In the constant chemical potential version of the algorithm, the last term in the previous equation is zero. However, we want to consider the case where the number of electrons is assumed constant for obtaining the force. This means that

$$\frac{\partial N}{\partial \vec{R}_n} = \text{Tr}\left[\frac{\partial F}{\partial \vec{R}_n}\right] = 0, \tag{A.15}$$

or substituting Eq. (A.13),

$$\text{Tr}\left[p'_{\mu,\tau}(H)\left(\frac{\partial H}{\partial \vec{R}_n} - \frac{\partial \mu}{\partial \vec{R}_n}\right)\right] = 0. \tag{A.16}$$

We can now solve for the derivative of the chemical potential:

$$\frac{\partial \mu}{\partial \vec{R}_n} = \frac{\text{Tr}[p'_{\mu,\tau}(H)(\partial H/\partial \vec{R}_n)]}{\text{Tr}[p'_{\mu,\tau}(H)]}. \tag{A.17}$$

Substituting into Eq. (A.14) gives the final force equation that we use

$$\vec{f}_n = -\text{Tr}\left[\frac{\partial H}{\partial \vec{R}_n}\left(p_{\mu,\tau}(H) + H p'_{\mu,\tau}(H)\right)\right] + \text{Tr}\left[p'_{\mu,\tau}(H)\frac{\partial H}{\partial \vec{R}_n}\right]\frac{\text{Tr}[H p'_{\mu,\tau}(H)]}{\text{Tr}[p'_{\mu,\tau}(H)]}. \tag{19}$$

These traces are then calculated in exactly the same manner as those for the band-structure energy, described earlier in Section A.1 of this appendix.

Another constant N_{elec} force calculation for this algorithm has been mentioned in [41], although to our knowledge the specifics of this algorithm have not been published.

References

[1] A. Ural, P.B. Griffin, J.D. Plummer, Appl. Phys. Lett. 73 (1998) 1706.
[2] H. Bracht, E.E. Haller, R. Clark-Phelps, Phys. Rev. Lett. 81 (1998) 393.
[3] P.M. Fahey, P.B. Griffin, J.D. Plummer, Rev. Mod. Phys. 61 (1989) 289.
[4] R.W. Dutton, A.G. Gonzalez, R.D. Rung, D.A. Antoniadis, in: H.R. Huff, E. Sirtl (Eds.), Semiconductor Silicon 1977, Proceedings of the Third International Symposium on Silicon Materials Science and Technology, The Electrochemical Society, Princeton, NJ, 1977, pp. 910–916.

[5] D.W. Yergeau, E.C. Kan, M.J. Gander, R.W. Dutton, in: H. Ryssel, P. Pichler (Eds.), Simulation of Semiconductor Devices and Processes, vol. 6, Springer, Wien, Austria, 1995, pp. 66–69.
[6] S. Dannefaer, P. Mascher, D. Kerr, Phys. Rev. B 56 (1986) 2195.
[7] Toshiharu K. Mogi, Point defect diffusion and dopant-defect interactions in Si (100) doping superlattices, Ph.D. Thesis, Cornell University, Ithaca, NY, 1996.
[8] G.H. Gilmer, T. Diaz de la Rubia, D.M. Stock, M. Jaraiz, Nucl. Inst. Meth. Phys. Res. B 102 (1995) 247.
[9] T. Sinno, Z.K. Jiang, R.A. Brown, Appl. Phys. Lett. 68 (1996) 3028.
[10] P.E. Blöchl, E. Smargiassi, R. Car, D.B. Laks, W. Andreoni, S.T. Pantelides, Phys. Rev. Lett. 70 (1993) 2435.
[11] G.D. Watkins, MRS Symp. Proc. 469 (1997) 139.
[12] V. Privitera, S. Coffa, K. Kyllesbech Larsen, S. Libertino, G. Mannino, F. Priolo, MRS Symp. Proc. 469 (1997) 163.
[13] P.A. Stolk, H.J. Gossmann, D.J. Eaglesham, J.M. Poate, Mater. Sci. Eng. B 36 (1996) 275.
[14] K.K. Larsen, P.A. Stolk, V. Privitera, J.G.M. van Berkum, W.B. de Boer, G. Mannino, N.E.B. Cowern, H.G.A. Huizing, Defects and Diffusion in Silicon Processing, MRS Symp. Proc. 469 (1997) 291.
[15] D. Maroudas, R.A. Brown, Appl. Phys. Lett. 62 (1993) 172.
[16] D. Maroudas, R.A. Brown, Phys. Rev. B 47 (1993) 15562.
[17] F.H. Stillinger, T.A. Weber, Phys. Rev. B 31 (1985) 5265.
[18] L. Goodwin, A.J. Skinner, D. Pettifor, Europhys. Lett. 9 (1989) 701.
[19] M. Tang, L. Colombo, J. Zhu, T.D. de la Rubia, Phys. Rev. B 55 (1997) 14279.
[20] I. Kwon, R. Biswas, C.Z. Wang, K.M. Ho, C.M. Soukoulis, Phys. Rev. B 49 (1994) 7242.
[21] L. Goodwin, A.J. Skinner, D.G. Pettifor, Europhys. Lett. 701 (1989) 9.
[22] A.P. Sutton, M.W. Finnis, D.G. Pettifor, Y. Ohta, J. Phys. C 21 (1988) 35.
[23] D.G. Pettifor, in: D.G. Pettifor, A.H. Cottrell (Eds.), Electron Theory in Alloy Design, The Institute of Materials, London, 1992, pp. 81–121.
[24] C.Z. Wang, K.M. Ho, in: I. Prigogine, S.A. Rice (Eds.), Advances in Chemical Physics, vol. XCIII, New Methods in Computational Quantum Mechanics, Wiley, New York, 1996, pp. 651–702.
[25] X.-P. Li, W. Nunes, D. Vanderbilt, Phys. Rev. B 47 (1993) 10891.
[26] M.S. Daw, Phys. Rev. B 47 (1993) 10895.
[27] S. Goedecker, L. Colombo, Phys. Rev. Lett. 73 (1994) 122.
[28] S. Goedecker, M. Teter, Phys. Rev. B 51 (1995) 9455.
[29] C.Z. Wang, C.T. Chan, K.M. Ho, Phys. Rev. Lett. 66 (1991) 189.
[30] W. Luo, P.B. Rasband, B.W. Roberts, P. Clancy, J. Appl. Phys. 84(5) (1998) 2476–2486.
[31] Paul B. Rasband, A Tight Binding study of formation and transport properties of defects in B-doped Si, Ph. D. Thesis, Cornell University, Ithaca, NY, 1996, pp. 215–220.
[32] G. Kresse, J. Hafner, Phys. Rev. B 47 (1993) 558.
[33] G. Kresse, J. Hafner, Phys. Rev. B 49 (1994) 14251.
[34] G. Kresse, J. Furthmüller, Comput. Mat. Sci. 6 (1996) 15.
[35] G. Kresse, J. Furthmüller, Phys. Rev. B 54 (1996) 11169.
[36] H. Soleimani, Digital Equipment Corporation, private communication, 1993.
[37] J. Zhu, Defects and diffusion in silicon precessing, MRS Symp. Proc. 469 (1997) 151.
[38] S.J. Clark, G.L. Ackland, Phys. Rev. B 56 (1997) 47.
[39] P.B. Rasband, P. Clancy, M.O. Thompson, J. Appl. Phys. 79 (1996) 8998.
[40] H. Hellmann, Einführung in die Quantenchemie, (Deuieke, Leipzig, 1937), R.P. Feynman, Phys. Rev. 56 (1939) 340.
[41] L.B. Hansen, K. Stokbro, B.I. Lundqvist, K.W. Jacobsen, D.M. Deaven, Phys. Rev. Lett. 75 (1995) 4444.
[42] M. Tang, L. Colombo, T. Diaz de la Rubia, MRS Symp. Proc. 396 (1996) 33.
[43] J.L. Mercer, J.S. Nelson, A.F. Wright, E.B. Stechel, Modelling Sim. Mat. Sci. Eng. 6 (1998) 1.